Received May 1999
Revised September 2000
Accepted September 2000

# Fluid flow and heat transfer in gas jet quenching of a cylinder

U. Heck, U. Fritsching and K. Bauckhage
*Institute for Material Science, Bremen, Germany*

***Keywords*** *Heat treatment, Gas jet, Heat transfer, Optimization*

***Abstract*** *Heat treatment by quenching of individual metallic parts with multiple impinging gas jets is an environmentally friendly alternative to conventional surface hardening and quenching in liquids. In the present investigation the gas flow field and simultaneous heat transfer process in gas quenching is studied by numerical simulation for surface treatment of a cylindrical sample geometry. Aim of the investigation is the evaluation of optimized flow conditions and nozzle arrangements to achieve: a maximum overall heat release (high integral heat transfer rates) to maximize the quenching efficiency; a local smooth distribution of the cooling process (spatially homogeneous heat transfer) for avoidance of spatial hardness variations. These aims are achieved by derivation of an optimized nozzle arrangement and appropriate operation conditions of the gas jet array with respect to the three dimensional sample geometry of a cylinder to be quenched.*

## Introduction

The flow field and heat or mass transfer resulting from an individual impinging gas jet or from an array of impinging gas jets has been studied in the past within a great number of investigations. Experimental or simulated data are collected and compared for single jets (e.g. in Jambunathan *et al*., 1992; Viskanta, 1993; Cooper *et al*., 1993; Craft *et al*., 1993; 1997; Behnia *et al*., 1999) and for gas jet systems (e.g. in Martin, 1977; Huber and Viskanta, 1994; Yang and Shyu, 1998; Arjocu and Liburdy, 2000). The listed recent publications represent only a small part of the relevant literature. A more complete listing may be found in the Jet Impingement Database at the Edinburgh Engineering Virtual Library (EEVL) at the Internet address http://www.eevl.ac.uk/jet/index.html. In this database over 1,200 abstracts from journals, proceedings, and papers may be found covering jet impingement phenomena and engineering applications for the transfer of energy and mass by action of a single-phase fluid on a surface.

Gas jet systems are used in several technical applications, e.g. for cooling or drying purposes. A rather new and interesting area of impinging gas jet applications for convective cooling is within the framework of heat treatment of metals: the flexible gas quenching of individual technical parts and components with gases. Due to recent efforts and developments in the area of environmental protection, which show evident problems of conventional metal quenching processes in oil or salt solutions especially in liquid bath regeneration and waste handling, the specific heat treatment process of gas jet quenching yielded a renewed interest. Within the process of flexible gas

International Journal of Numerical Methods for Heat & Fluid Flow, Vol. 11 No. 1, 2001, pp. 36-49.

quenching of technical parts or components, specifically to the geometry of each sample, adapted gas jet arrays are used for blowing gas onto the heated surface, resulting in rapid convective cooling by the gas flow. A reasonably high cooling rate may result in a specific phase change of the metal and a martensitic hardening of the surface. Therefore, a flexible geometric arrangement of the array for hardening of different part geometries as well as suitable operational parameters of the gas jet system are needed.

In Figure 1, the principle arrangement of a flexible gas quenching process for a cylindrical sample is illustrated. In the centre of the device the sample is fixed. A number of gas jets from individual nozzles is directed in radial direction (and sometimes simultaneously from the top and bottom end of the domain) onto the sample surface. The flow field results in a principle distribution of the heat transfer coefficient which is sketched in the figure on the right: in the stagnation point area of each jet a local maximum of the heat transfer can be seen (assuming a sufficient minimal distance between jet exit and impingement plane).

For the derivation of optimized flow conditions, the geometric parameters of the gas jet array are changed in numerical calculations. These parameters are:

- the spacing between the jets in axial and circumferential direction ($t_{ax}$ and $t_{rad}$); and
- the distance $h$ between the nozzle exit plane and the surface of the sample.

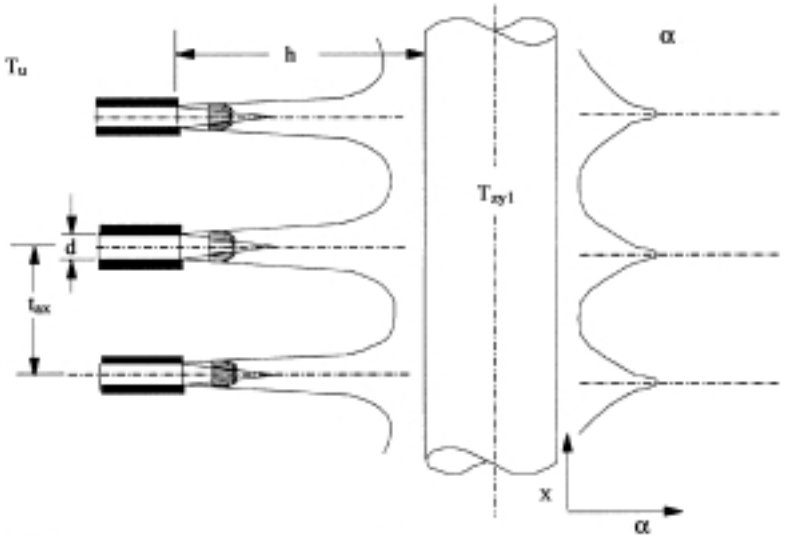


**Figure 1.**
Principle of flexible sample quenching by gas jets (left: nozzle arrangement and flow field; right: heat transfer coefficient distribution)

An optimized flow field configuration is defined as resulting in a maximum integral heat transfer with a minimum in spatial variations of the heat transfer coefficient. The maximum integral heat transfer should be achieved for an overall rapid quenching process, the local smoothness of the heat transfer distribution is needed for minimizing spatial hardness variations as well as stresses and deformations (distortion) in the sample material during the quenching process.

In the numerical modelling of the combined flow and heat transfer process of impinging gas jets, the transfer of the physical behaviour and boundary conditions into a numerical model is of significant importance. Especially the suitable description of the turbulent flow and heat transfer close to the stagnation point and in the close wall regions needs special care. In the region close to the stagnation point of each impinging gas jet, pressure gradients result and the flow is not in local equilibrium. Therefore, the assumption and application of standard logarithmic velocity profiles and appropriate boundary conditions in terms of wall laws for velocity distribution (log-law, derived from boundary layer theory in the turbulent region of the flow field) are in question.

In the first part of the investigation, the numerical analysis of a single impinging circular gas jet on a plane surface is performed and will be discussed for necessary assessment and modifications of the model assumptions. In the second part, the application of the model and configuration to a three dimensional array of impinging gas jets for the sample geometry of a cylinder are discussed.

## Model assumptions

For numerical simulation of the coupled gas flow and heat transfer problem of impinging jets, the equations for conservation of mass (continuity equation), conservation of momentum in combination with an appropriate turbulence model and conservation of thermal energy have to be solved. In the literature different turbulence models as standard two-equation models ($k$-$\epsilon$ and variations herefrom), low-Reynolds number models, algebraic stress models, nonlinear eddy viscosity models or higher order closures as Reynolds stress models have been used and compared. The deviations of some models to experimental values are remarkable. Due to the complex nature of the flow in impinging jets, this flow configuration recently has been chosen as a turbulence model test case which has been calculated by several groups. The data are published in the ERCOFTAC database at http://ercoftac.mech.surrey.ac.uk No general or simple conclusion about the "best" turbulence model for a specific technical application and flow situation can be made. The decision depends on reflection of the specific application and physical frame (general geometry, Reynolds number range, . . .) and the accuracy to be achieved, keeping in mind the necessary computer power as well as the availability of the specific model.

In the present contribution the Renormalization-Group (RNG-k-$\epsilon$) turbulence model (Yakhot *et al.*, 1992; Yakhot and Orszag, 1986) is applied. In a prior study this model was found to reflect the basic features of the impinging jet flow in

the near wall region and impingement region adequately (Heck and Fritsching, 1995). The RNG model may serve as a good compromise between accuracy and effort for some three dimensional flow field calculations. In this two equation model the conservation equations for the turbulent kinetic energy $k$ and its dissipation rate $\varepsilon$ are:

$$\rho \frac{dk}{dt} = \frac{\partial}{\partial x_i}\left(\alpha_k \mu_{eff} \frac{\partial k}{\partial x_i}\right) + G_k + G_b - \rho\varepsilon$$

$$\rho \frac{d\varepsilon}{dt} = \frac{\partial}{\partial x_i}\left(\alpha_\varepsilon \mu_{eff} \frac{\partial \varepsilon}{\partial x_i}\right) + C_{1\varepsilon}\frac{\varepsilon}{k}(G_k + C_{3\varepsilon} G_b) - C_{2\varepsilon}\rho\frac{\varepsilon^2}{k} - R$$

where $\alpha_k$ is the inverted effective Prandtl number for $k$ and $\alpha_\epsilon$ is the inverted effective Prandtl number for $\epsilon$. The source terms $G_k$ and $G_b$ describe the production of turbulence due to shear gradients and buoyancy. For low Reynolds number conditions the effective viscosity $\mu_{eff} / \mu$ is derived from:

$$d\left(\frac{\rho^2 k}{\sqrt{\varepsilon\mu}}\right) = 1.72 \frac{\mu_{eff}/\mu}{\sqrt{(\mu_{eff}/\mu)^3 - 1 + C_\mu}} d(\mu_{eff}/\mu)$$

with the model constants $C_{1\epsilon} = 1.42$; $C_{2\epsilon} = 1.68$; $C_{3\epsilon} = 0.2$; $C_\mu = 0.0845$. The RNG turbulence model is more sensitive to the effects of rapid strain and streamline curvature than the conventional $k$-$\epsilon$ model due to the formulation of the R-term in the dissipation equation. This term reads:

$$R = \frac{c_\mu \rho \eta^3 (1 - \eta/\eta_0)}{1 + \beta \eta^3} \frac{\varepsilon^2}{k}$$

where $\eta = S k / \epsilon$ with $S$ the modulus of the mean strain rate; $\eta_0 = 4.38$; $\beta = 0.012$.

The solution of the discretized conservation equations is done within the FLUENT code (FLUENT, 1996). A second order upwind scheme for convection terms and central differences for diffusion terms is used. A general curvilinear coordinate system with a structured grid system has been used to reflect the complex geometric situation. The grid independency of the solution has been checked by subsequent refinement of the near wall region in a two dimensional jet impingement calculation. At a level of 35 grid nodes used to resolve the normal wall distance of 1.5 nozzle diameters a further refinement did not achieve any mayor improvements of the solution in good agreement with experimental values.

In addition to the general model formulation, boundary conditions and especially the boundary layer treatment at the wall for velocity and temperature are of importance. In the flow field close to the solid wall, the hydrodynamic and thermal wall boundary layer is established, which can be divided into the region of the viscous sublayer and a fully developed turbulent

region at some distance to the wall. The interface between these regions can be characterized in equilibrium boundary layers by the value of the dimensionless wall distance (Jayatilleke, 1969) $y_0{}^+ \sim 11.25$. Here, the wall distance $y^+$ is nondimensionalized by the shear velocity $u_\tau$ as $y^+ = y\ u_\tau/\nu$ Models which resolve the total boundary layer (e.g. low-Reynolds number models) need a huge number of grid points in that area. In three dimensional calculations this may exceed the computer storage which is on hand. In some numerical models for heat transfer incorporating wall functions, the transition of the thermal sublayer to the fully turbulent temperature boundary layer is related to the thickness of the hydrodynamic boundary sublayer $y_0{}^+$ by a constant factor, the turbulent Prandtl-number. In widely used two equation turbulence eddy viscosity models like the standard $k$-$\epsilon$ model or the Renormalization Group Model (RNG-model) based on Boussinesq's approximation and principle of apparent turbulent viscosity, the vicinity of the wall in the viscous sublayer is not solved explicitly but bridged by some approximations. Therefore, the nearest grid point with respect to the wall must be located in the fully turbulent region. The shear velocity $u_\Upsilon$ is derived from the turbulent kinetic energy value in this grid point $k_p$ based on the assumption, that in this region the viscous stresses are small compared to the turbulent (Reynolds) stresses as: $u_\tau = C_\mu{}^{1/4} k_P{}^{1/2}$ with the model constant $C_\mu$ of the $k$-$\epsilon$ model.

In the fully developed turbulent region of a boundary layer, the universal logarithmic wall law for temperature and velocity profiles is derived. In combination, the specific heat transfer flux can be calculated based on (Launder and Spalding, 1974):

$$\dot{q}''_w = \frac{(T_w - T_p)\rho\, c_p\, C_\mu{}^{1/4}\, k_p{}^{1/2}}{Pr_t[\frac{1}{\kappa}\ln(E\, y_p{}^+ P)]}$$

$$P = 9.24\left[\left(\frac{Pr}{Pr_t}\right)^{3/4} - 1\right]\left[1 + 0.28\exp\left(-0.007\,\frac{Pr}{Pr_t}\right)\right]$$

In this correlation, the driving temperature difference between the wall temperature and the gas temperature at the point closest to the wall is ($T_W$–$T_P$), the material properties of the gas are density $\rho$ and heat capacity $c_p$, the shear velocity is $u_\tau = C_\mu{}^{1/4}\, k_P^{1/2}$ and the turbulent Prandtl-number is $Pr_t$. The expression $P$ is an empirical function (Jayatilleke, 1969), describing additional effects of wall surface roughness. The advantage of the usage of wall functions as boundary conditions in the numerical simulation is that the viscous sublayer need not be resolved in a grid system, which makes the numerical model rather robust and saves grid points in the wall vicinity.

An alternative to the calculation of turbulent flows with wall laws is the resolution of the viscous sublayer in wall bounded flows and boundary layers as in low-Reynolds number-$k$-$\epsilon$ models. The investigation of Djilali *et al.* (1989) on different turbulence models and different wall approximations for calculation of the heat transfer in a backward facing step flow compared to

experimental results yields the best results for a three zone model for boundary layer resolution. Here, the viscous sublayer in the region $y^+ < 5$, the buffer layer for $5 < y^+ < 30$ and the fully developed turbulent region $30 < y^+ < 400$ are all resolved in the numerical grid system. Due to the necessary high resolution of the grid system in the wall vicinity, these models resolve the boundary layer and describe the transport and exchange of momentum and thermal energy in the boundary layer more exactly in a physical view but are difficult to use with respect to a three dimensional model calculation which is intended here. The necessary computer power exceeds the existing capacity by far. Therefore, an extension of the concept of the log-laws of the wall is applied in the present approximation.

**Heat transfer modelling in turbulent flow of an impinging jet**

In a first approximation, two dimensional model calculations for a cylindrical jet impinging perpendicular onto a flat surface (assuming circumferential symmetry) have been performed by means of the RNG $k$-$\epsilon$ model for turbulence modelling. Here the aforementioned wall boundary conditions for the heat transfer have been used. The stationary flow field is calculated assuming a constant wall temperature. The local heat transfer coefficient is calculated from the heat flux distribution with respect to the temperature difference between the jet and the wall. Therefore, a local Nusselt number can be derived as:

$$Nu_{lo}(r) = \frac{\dot{q}''(r)\,d}{(T_w - T_d)\lambda} = \frac{\alpha(r)\,d}{\lambda}$$

The distance between the nozzle and the impingement plane was chosen to a value of twice the nozzle exit diameter in this calculation ($h/d = 2$). At this relatively small distance from the jet exit to the wall, a remarkable deviation between numerical simulation results and experimental results often can be found in literature. In Figure 2, the comparison between experimental results from literature (Goldstein *et al.*, 1986; Huang and El-Genk, 1994) and results from our numerical calculation are illustrated. The measurements are at comparable Reynolds numbers based on nozzle exit diameter and velocity:

$$Re_d = \frac{\rho \nu_d\, d}{\eta}$$

The abcissa of Figure 2 represents the dimensionless radius, the origin is the stagnation point. The ordinate gives the normalized heat transfer in terms of the Nusselt number. By normalization of the heat transfer coefficient with respect to the nozzle Reynolds number, different operational conditions and gas jet configurations can be compared within a single representation.

For radial distances $r/d > 2$ from the stagnation point, results of the computed heat tansfer coefficients are in good agreement with the experimental results. Nevertheless, in the region close to the stagnation point the comparison shows some deviations. One problem in calculation of turbulent boundary

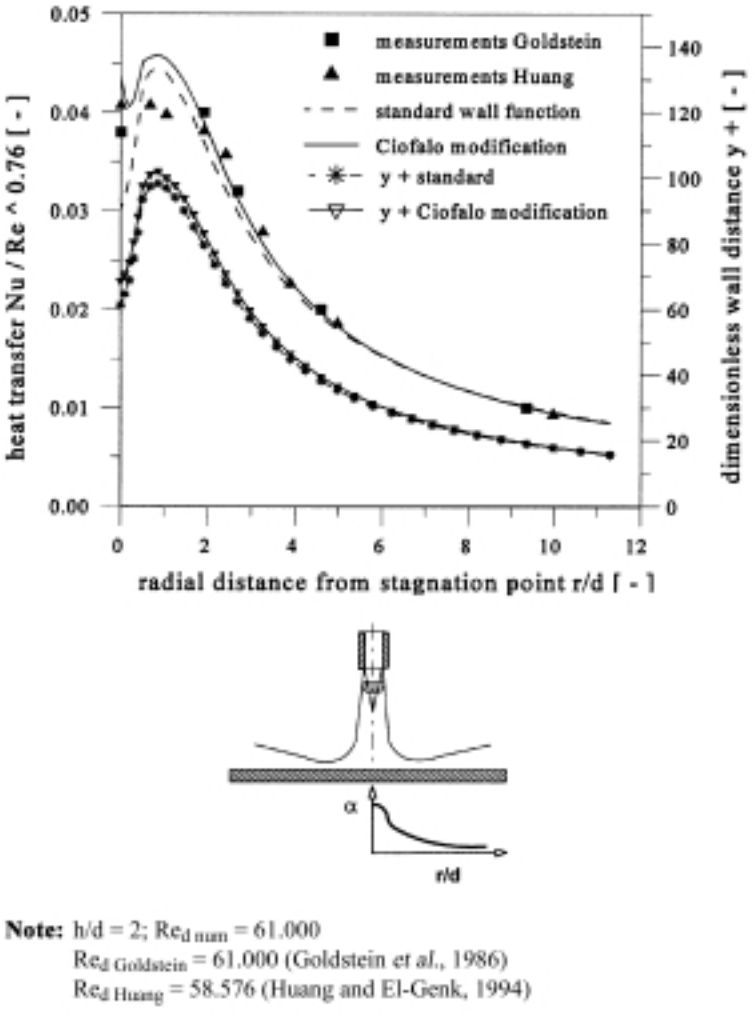


**Note:** h/d = 2; $Re_{d\,num}$ = 61.000
$Re_{d\,Goldstein}$ = 61.000 (Goldstein *et al.*, 1986)
$Re_{d\,Huang}$ = 58.576 (Huang and El-Genk, 1994)

**Figure 2.**
Distribution of the normalised Nusselt number and dimensionless wall distance for a single jet in comparison to measurements

layers is the dependence of the solution on the grid distribution. Therefore, in addition to the calculated heat transfer coefficients, the distribution of the dimensionless wall distance $y^+$ of the grid node closest to the wall has to be considered ($y^+ = y_P u_\tau / \nu$). Due to the strong increase of the shear velocity in the stagnation region, the $y^+$ values also increase for radial distances of $r/d = 1$ in a grid system with constant spacing to the wall. This behaviour does not meet the necessary physical assumption and boundary condition of the turbulence model, that the grid point closest to the wall has to be at a distance of $30 < y^+ < 60$, whereas the distance for the logarithmic velocity wall law is $30 < y^+ < 100$.

Because the usage of standard log-laws yields some deviations in the stagnation region, several modifications of the wall laws in turbulent flows

have been tested and applied to the case of the single impinging jet. A modification derived for the stagnation region of a backward facing step flow was derived by Ciofalo and Collins (1988; 1989). The basic assumption of this model is that the boundary layer is not fully developed in the stagnation region and that a local variable thickness of the viscous sublayer has to be defined as:

$$\frac{y_c^+}{y_0^+} = \left(\frac{\Psi_p}{\Psi_E}\right)^{-0,5}.$$

In the Ciofalo concept, the transition value from the viscous sublayer to the fully turbulent region $y_c^+$ is not a constant as in a fully developed boundary layer ($y_0^+ = 11.25$) but is derived from the local distribution of turbulence intensities $\Psi$. The turbulence intensity in the grid point closest to the wall $\Psi_p$ is calculated from $\Psi_p = k_p^{0.5} / u_p$ and $\Psi_E$ is the modified turbulence intensity based on the local Reynolds number. The ratio $\Psi_p / \Psi_E$ can be seen as the deviation of the actual local flow field from the fully developed stage of a turbulent boundary layer. This boundary condition modification has been introduced into the FLUENT code by user defined subroutines.

The calculation with the modification yields higher values of heat transfer in the stagnation point in better agreement with the measurements. The off-centre maximum is calculated slightly higher than in the standard model. As the distance to the stagnation point increases, the agreement of the calculated values with the modification yields slightly better values than with the standard model when compared to the measured values. The distribution of the dimensionless wall distance $y^+$ shows higher values with the modification than with the standard function.

By using the Ciofalo modification of the boundary conditions at the wall, the calculation of the heat transfer coefficient yields slightly better results than the standard wall functions in the stagnation point which is a critical point in all numerical jet calculations. For the derivation of the logarithmic wall functions a constant pressure distribution is assumed, but strong pressure gradients exist in the stagnation area of the impinging jet (where deviations of the calculated values from measurements are found). Nevertheless, the principal agreement of the calculated heat transfer data with experiments is sufficient and allows the assessment for the case of multiple, interacting jets.

The main aim of this investigation is the finding and evaluation of an optimized nozzle arrangement in a jet array for gas quenching of complex samples with respect to the maximization of the overall heat transfer by simultaneously minimizing local changes in heat transfer from the sample surface. As a basic geometry the quenching process of a circular cylinder is studied. The calculations are performed assuming a constant wall temperature. The heat transfer behaviour will be described by means of the distribution of the local Nusselt number and the integral Nusselt number:

$$Nu_{integ} = \frac{\sum Nu_{lo}(x,y)\triangle A}{A_{tot}},$$

describing the overall heat flux from the cylinder surface to the gas.

## Results for the cylinder

The calculated flow field for the three dimensional flow around a cylinder is shown in Figure 3 in the form of shaded velocity contours. The cylinder is located in the centre of the figure, the gas jet array is radially directed onto the sample surface. Due to symmetry conditions, for the radial spacing of $t_{rad}$ = 25.7° of the jets shown here, a sector of 90° was resolved and calculated in the three dimensional grid system. The axial nozzle spacing is close in this case, the distance between the nozzles is $t_{ax}/d$ = 2. The tips of the nozzle system are located close to the probe surface at a dimensionless distance of $h/d$ = 4. In the right part of the figure, the view at a slice through the nozzles is illustrated. At the left, the plane between the nozzles is shown and in the lower part of the figure the radial plane through the nozzles is to be seen. The Reynolds number for each nozzle is $Re_d$ = 17,000. Due to the relatively close spacing of the nozzles, the interaction between the jets is evident and a rapid mixing area of the jets results above the cylinder surface where the jets intermingle and lose their individual identity. The close jet spacing hinders the exhaust flow of the gas between the nozzles. The main outflow occurs over the top and low end

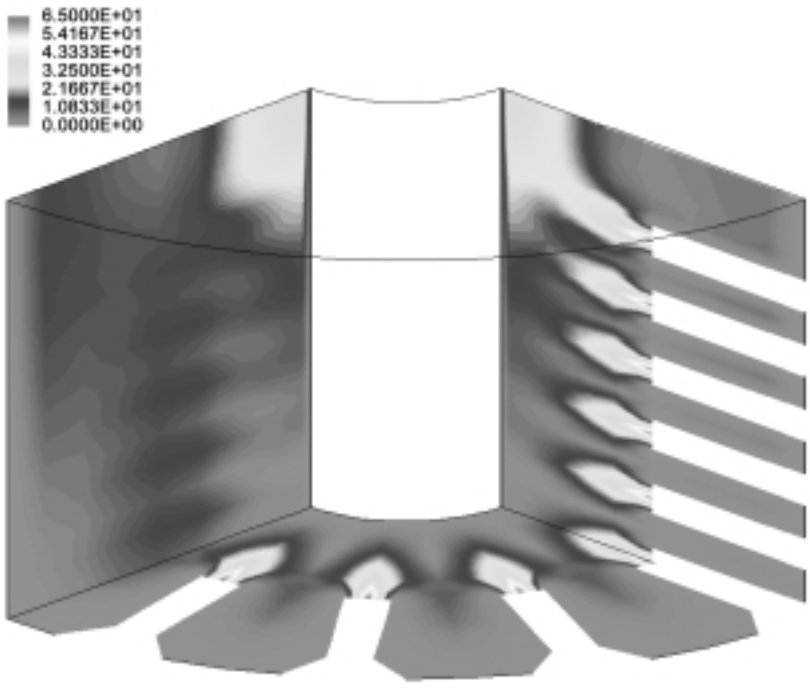


**Figure 3.**
Velocity distribution for a cylinder in a gas jet system; $h/d$ = 4, $t_{ax}$/d =2, $t_{rad}$ = 25.7°, $Re_d$ = 17,000

sides of the domain, only a small portion of the gas exits over the circumference in between the jets. This jet interaction results in relatively low velocity values in the boundary layer at the cylinder surface.

The gas flow field and velocity distribution resulting from a simulation at a coarser spacing of the nozzle arrangement is shown in Figure 4. Here, only seven nozzles remain in the jet arrangement for a circumferential spacing of $t_{rad}$ = 51.4°. The number of jets in axial direction is also divided by two ($t_{ax}/d$ = 4). In this case, the flow field within a 180° segment is actually calculated in the simulation and shown in the figure. At this increased spacing of the jets, the interaction of the jets is small and the individual jet flow reaches the cylinder surface. Also the flow can be exhausted more easily in between the nozzles. Therefore, the absolute value of the gas velocity at the cylinder surface is increased, but also the relative fluctuations of the heat transfer coefficient are increased as can be seen in Figure 5. Here, the calculated distribution of the local Nusselt number on the developed cylinder surface is shown for that case ($h/d$ = 4; $t_{ax}/d$ = 4; $t_{rad}$ = 51.4°), which results in distinct maxima in the stagnation point of each jet and minima in the area half way between the stagnation points. The ratio of the maximum to the minimum heat transfer coefficient value is app. 4.

The distributions of the local Nusselt number over the cylinder height on a line immediately under a row of nozzles for a constant nozzle distance to the

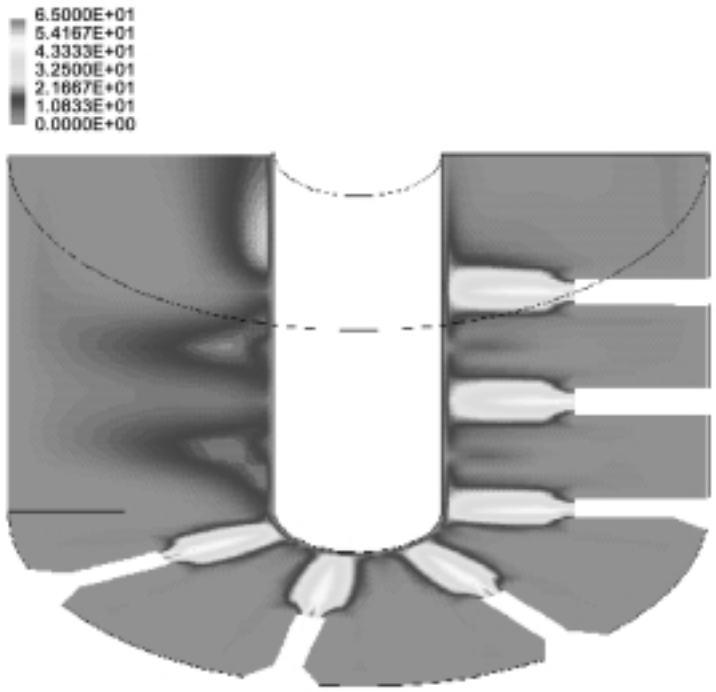


**Figure 4.**
Velocity distribution for a cylinder in a gas jet system; $h/d$ = 4, $t_{ax}$/d = 4, $t_{rad}$ = 51.7°, $Re_d$ = 17,000

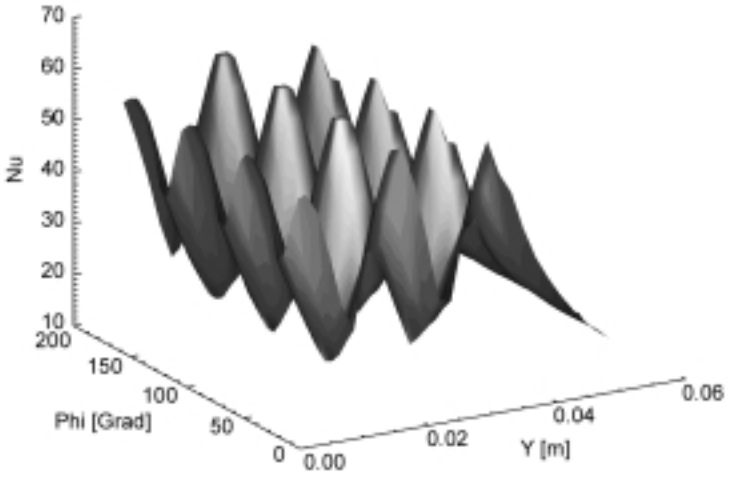


**Figure 5.**
Local Nusselt number for the cylinder sample; $h/d$ =4, $t_{ax}/d$ = 4, $t_{rad}$ = 51.7°, $Re_d$ = 17.000

cylinder of $h/d$ = 4 and for different nozzle spacings are compared in Figure 6. A narrow distribution of the jets ($t_{ax}/d$ = 2; $t_{rad}$ = 25.7°) results in relatively homogeneous velocity distributions in the boundary layer with low local variations of the heat transfer coefficient but also low values of the overall heat transfer. At increased nozzle spacings ($t_{ax}/d$ = 4; $t_{rad}$ = 51.4°), high variations of the heat transfer coefficient results in a heat transfer maximum below each nozzle. At further increased nozzle spacings, the Nusselt number decreases due to the reduction in the overall gas mass flow rate with the decreasing number of nozzles in the array for a constant nozzle exit velocity.

Calculated values of the integral Nusselt number describing the total heat release of the cylinder surface are shown in Figure 7 for various nozzle spacings at a constant nozzle to cylinder distance of $h/d$ = 4. The calculated

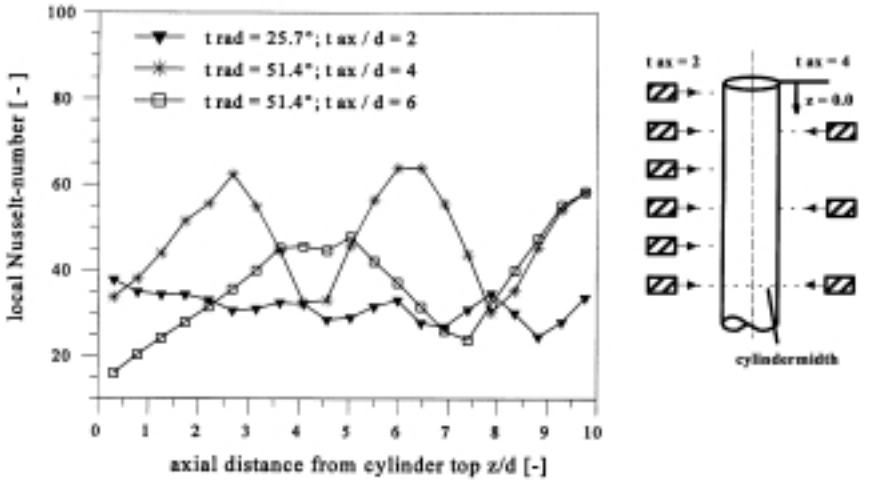


**Figure 6.**
Local Nusselt number for cylinder; $h/d$ = 4, $Re_d$ = 17,000

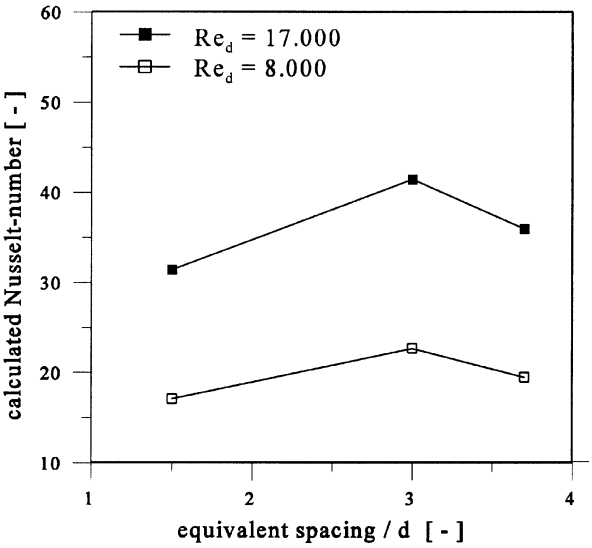


**Figure 7.**
Integral Nusselt number for cylinder; $h/d = 4$

equivalent spacing for different radial and axial spacings refers to the free distance between two individual jets. At narrow spacings between the nozzles, mixing of the jets results in a decreased integral Nusselt number, reflecting the behavior of the local Nusselt number shown before. Because these results are achieved for constant jet exit velocities of the gas, the decrease of nozzle spacing is directly proportional to a decrease of the total mass flow rate for cooling. As can be seen from the figure, despite a decrease of total mass flow rate at $t_{eq}/d = 3$ ($t_{ax}/d = 4$; $t_{rad} = 51.4°$) to 25 per cent of the mass flow rate at $t_{eq} = 1.6$ ($t_{ax}/d = 2$; $t_{rad} = 25.7°$), an increased overall heat transfer is achieved. By further increasing of the nozzle spacing, the total heat release decreases again, because the mass flow rate decreases and no further optimized conditions for the interaction of the gas jets can be realized compared to an equivalent spacing of three. This principal behaviour was reproduced for different values of the gas exit velocity. Variations in gas exit velocities only shift the curve without changing its principal qualitative behaviour as can be seen also in Figure 7 for $Re_d = 8{,}000$.

## Summary and conclusions

The numerical simulation of the heat transfer process resulting from the impingement of a single cylindrical gas jet at small distances between the nozzle and the surface has shown, that the RNG-$k$-$\epsilon$ model in combination with modified boundary conditions for turbulent flow field and heat transfer calculations (Ciofalo and Collins, 1988; 1989) can improve the calculated results for the heat flux value in the stagnation area and yield reasonable agreement with literature data of single impinging jets. Directly at the stagnation point, better agreements to experimental data are achieved by this modification.

The three dimensional simulation of the impingement process of a multiple jet array shows the complex behaviour of the gas flow and the resulting heat transfer from a cylindrical sample for varying nozzle arrangements. With these calculations, the geometric arrangement of the jet array can be economically optimized for a reduction of gas consumption in a gas quenching process. Therefore, the main aim of the investigation of numerical calculation of the heat transfer process as a tool for optimization of flexible heat treatment processes is achieved. In particular, the simulation helps to explain fundamental transport processes in the flow field. Here the onset of the mixing area between the jets with respect to the geometric arrangement (e.g. for the cylinder quenching) of the jet array is determined and visualized.

**References**

Arjocu, S.C. and Liburdy, J.A. (2000), "Indentification of dominant heat transfer modes associated with the impingement of an elliptical jet array", *J. Heat Transfer*, Vol. 122, pp. 240-7

Behnia, M., Parneix, S., Shabany, Y. and Durbin, P.A. (1999), "Numerical study of turbulent heat transfer in confined and unconfined impinging jets", *Int. J. Heat and Fluid Flow*, No. 20, pp. 1-9

Ciofalo, M. and Collins, M.W. (1988), "Predictive study of heat transfer to an incompressible fluid past a downstream step in turbulent flow", *Heat and Technology*, Vol. 6 No. 3-4, pp. 8-33.

Ciofalo, M. and Collins, M.W. (1989), "K-$\varepsilon$ predictions of heat transfer in turbulent recirculating flows using an improved wall treatment", *Numerical Heat Transfer, Part B*, No. 15, pp. 17-21.

Cooper, D., Jackson, D.C., Launder, B.E. and Liao, G.X. (1993), "Impinging jet studies for turbulence model assessment – I. Flow-field experiments", *Int. J. Heat Mass Transfer*, Vol. 36 No. 10, pp. 2675-84.

Craft, T.J., Graham, J.W. and Launder, B.E. (1993), "Impinging jet studies for turbulence model assessment - II. An examination of the performance of four turbulence models", *Int. J. Heat Mass Transfer*, Vol. 36 No. 10, pp. 2685-97.

Craft, T.J., Launder, B.E. and Suga, K. (1997), "Prediction of turbulent transitional phenomena with a nonlinear eddy-viscosity model", *Int. J. Heat and Fluid Flow*, Vol. 18, pp. 15-28.

Djilali, N., Garthsore, I. and Salcudean, M. (1989), "Calculation of convective heat transfer in recirculation turbulent flow using various near-wall turbulence models", *Numerical Heat Transfer, Part A*, No. 16, pp. 189-212.

FLUENT (1996), *User Guide Release 4.0*, Fluent Inc., Lebanon, PA.

Goldstein, R.J., Behbahani, A.I. and Krieger Heppelmann, K. (1986), "Streamwise distribution of recovery factor and local heat transfer coefficient to an impinging circular air jet", *Int. J. Heat Mass Transfer*, Vol. 29 No. 8, pp. 1127-235.

Heck, U. and Fritsching, U. (1995), "Berechnung des Wärmeübergangs an von Düsensystemen senkrecht angeströmten ebenen Flächen", *Proc. AEA 2. CFDS User Meeting*, 19-20 September, Stuttgart.

Huang, L. and El-Genk, M. (1994), "Heat tansfer of an impinging jet on a flat surface", *Int. J. Heat Mass Transfer*, Vol. 37 No. 13, pp. 1915-23.

Huber, A.M. and Viskanta, R. (1994), "Effect of jet-jet spacing on convective heat transfer to confined, impinging arrays of axisymmetric jets", *J. Heat Mass Transf.*, Vol. 37 No. 18, pp. 2859-69.

Jambunathan, K., Lai, E., Moss, M. and Button, B. (1992), "A review of heat transfer data for single circular jet impingement", *Int. J. Heat and Fluid Flow*, No. 13, pp. 106-15.

Jayatilleke, C.L.V. (1969), "The influence of Prandtl number and surface roughness on the resistance of the laminar sublayer to momentum and heat transfer", *Progress in Heat and Mass Transfer*, No. 1, pp. 193-329.

Launder, B.E. and Spalding, D.B. (1974), "The numerical computation of turbulent flows", *Computer Methods in Applied Mechanics and Engineering*, Vol. 3, pp. 269-89.

Martin, H. (1977), "Heat and mass transfer between impinging gas jets and solid surfaces", *Adv. Heat Transfer*, No. 13, pp. 1-60.

Viskanta, R. (1993), "Heat transfer to impinging isothermal gas and flame jets", *Exp. Thermal Fluid Sci.*, Vol. 6, pp. 111-34.

Yakhot, V. and Orszag, S.A. (1986), "Renormalization group analysis of turbulence", *J. Sci. Comput.*, Vol. 1.

Yakhot, V., Orszag, S.A., Thangam, S., Gatski, T.B. and Speziale, C.G. (1992), "Development of turbulence models for shear flows by a double expansion technique", *Phys. Fluids A*, Vol. 4 No. 7.

Yang, Y.-T. and Shyu, C.-H. (1998), "Numerical study of multiple impinging slot jets with an inclined confinement surface", *Num. Heat Transfer, Part A*, No. 33, pp. 23-37.